











OPEN ACCESS

Original research

MRI and CT coronary angiography in survivors of COVID-19

Trisha Singh ^{1,2,3} Thomas A Kite ⁴ Shruti S Joshi ^{1,2} Nick B Spath ^{1,2}
Lucy Kershaw,^{3,5} Andrew Baker,¹ Helen Jordan,⁶ Gaurav Singh Gulsin,⁴
Michelle Claire Williams ^{1,3} Edwin J R van Beek,^{1,3} Jayanth Ranjit Arnold,⁴
Scott I K Semple,³ Alastair James Moss ⁴ David E Newby ^{1,2,3} Marc Dweck,^{1,2,3}
Gerry P McCann ⁴

► Additional supplemental material is published online only. To view, please visit the journal online (<http://dx.doi.org/10.1136/heartjnl-2021-319926>).

For numbered affiliations see end of article.

Correspondence to

Dr Trisha Singh, BHF Centre for Cardiovascular Science, The University of Edinburgh, Edinburgh, Edinburgh, UK; tsingh@ed.ac.uk

TS and TAK contributed equally.

Received 25 June 2021

Accepted 10 September 2021

Published Online First

6 October 2021



► <http://dx.doi.org/10.1136/heartjnl-2021-320246>



© Author(s) (or their employer(s)) 2022. Re-use permitted under CC BY-NC. No commercial re-use. See rights and permissions. Published by BMJ.

To cite: Singh T, Kite TA, Joshi SS, *et al.* *Heart* 2022;**108**:46–53.

ABSTRACT

Objectives To determine the contribution of comorbidities on the reported widespread myocardial abnormalities in patients with recent COVID-19.

Methods In a prospective two-centre observational study, patients hospitalised with confirmed COVID-19 underwent gadolinium and manganese-enhanced MRI and CT coronary angiography (CTCA). They were compared with healthy and comorbidity-matched volunteers after blinded analysis.

Results In 52 patients (median age: 54 (IQR 51–57) years, 39 males) who recovered from COVID-19, one-third (n=15, 29%) were admitted to intensive care and a fifth (n=11, 21%) were ventilated. Twenty-three patients underwent CTCA, with one-third having underlying coronary artery disease (n=8, 35%). Compared with younger healthy volunteers (n=10), patients demonstrated reduced left (ejection fraction (EF): 57.4±11.1 (95% CI 54.0 to 60.1) versus 66.3±5 (95% CI 62.4 to 69.8%); p=0.02) and right (EF: 51.7±9.1 (95% CI 53.9 to 60.1) vs 60.5±4.9 (95% CI 57.1 to 63.2%); p≤0.0001) ventricular systolic function with elevated native T1 values (1225±46 (95% CI 1205 to 1240) vs 1197±30 (95% CI 1178 to 1216) ms; p=0.04) and extracellular volume fraction (ECV) (31±4 (95% CI 29.6 to 32.1) vs 24±3 (95% CI 22.4 to 26.4%); p<0.0003) but reduced myocardial manganese uptake (6.9±0.9 (95% CI 6.5 to 7.3) vs 7.9±1.2 (95% CI 7.4 to 8.5) mL/100 g/min; p=0.01). Compared with comorbidity-matched volunteers (n=26), patients had preserved left ventricular function but reduced right ventricular systolic function (EF: 51.7±9.1 (95% CI 53.9 to 60.1) vs 59.3±4.9 (95% CI 51.0 to 66.5%); p=0.0005) with comparable native T1 values (1225±46 (95% CI 1205 to 1240) vs 1227±51 (95% CI 1208 to 1246) ms; p=0.99), ECV (31±4 (95% CI 29.6 to 32.1) vs 29±5 (95% CI 27.0 to 31.2%); p=0.35), presence of late gadolinium enhancement and manganese uptake. These findings remained irrespective of COVID-19 disease severity, presence of myocardial injury or ongoing symptoms.

Conclusions Patients demonstrate right but not left ventricular dysfunction. Previous reports of left ventricular myocardial abnormalities following COVID-19 may reflect pre-existing comorbidities.

Trial registration number NCT04625075.

INTRODUCTION

In patients with COVID-19, there remains major concern surrounding the extent of cardiac involvement and its consequences. Myocardial injury is common in patients hospitalised with COVID-19 and correlates with disease severity and poor clinical outcomes.^{1–3} The mechanisms underlying this are not well understood, with some suggesting indirect mechanisms of injury similar to that of other severe respiratory illnesses.^{2,4–9} Others have proposed direct myocardial injury due to myocarditis, stress cardiomyopathy, endothelial injury, thromboinflammation or the result of profound ongoing myocardial oxygen supply or demand imbalance.^{5,10–14}

There are increasing reports of persistent and prolonged multiorgan effects after acute COVID-19 illness.^{15,16} More importantly, many patients continue to have debilitating symptoms during recovery,¹⁶ and it is important to understand whether cardiac damage observed in the acute phase of COVID-19 will translate into subsequent cardiac dysfunction and morbidity. Widespread myocardial abnormalities seen on cardiac MRI have been reported in patients with COVID-19.^{8,10–12} However, a large proportion of these patients have comorbidities, and the presence of coronary artery disease had not been excluded. It is therefore essential to understand whether such cardiac abnormalities are the result of underlying comorbidities or the direct impact of COVID-19.

Manganese-enhanced MRI has shown promise in assessing myocardial calcium handling¹⁷ and may measure more subtle disturbances in myocardial function. Using both gadolinium and manganese-enhanced MRI combined with CT coronary angiography, we sought to determine the contribution and impact of pre-existing cardiovascular disease on the cardiac abnormalities of patients recovering from COVID-19 hospitalisation.

METHODS

Written informed consent was obtained from all participants.

Participants

Adult patients recovering from hospitalisation with COVID-19 were recruited prospectively from the Edinburgh Heart Centre between May 2020 and November 2020 and Glenfield Hospital, Leicester

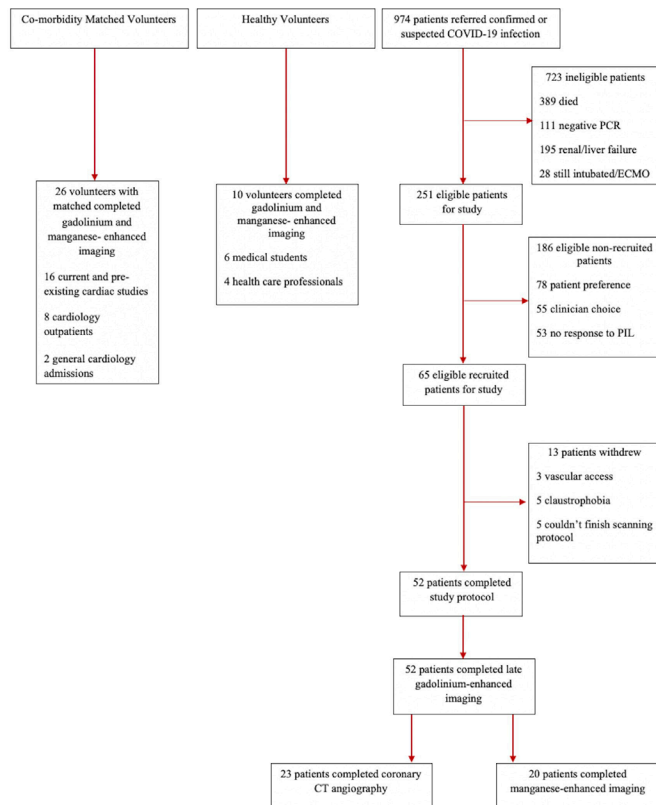


Figure 1 CONSORT diagram. CONSORT, Consolidated Standards of Reporting Trials; CTCA, CT coronary angiography; ECMO, extracorporeal membrane oxygenation; PIL, patient information leaflet.

between November 2020 and February 2021. The diagnosis of COVID-19 was based on a positive PCR test. Comparisons were made with healthy volunteers (10 participants) and volunteers matched for age, sex and comorbidities (26 participants). Patients and comorbid volunteers were propensity matched 1:2 to cardiovascular risk factors including hypertension, known ischaemic heart disease, hypercholesterolaemia and diabetes mellitus. Matched volunteers were recruited from general cardiology admissions, outpatient clinic or those recruited for other cardiac studies. The latter control group were scanned at Glenfield Hospital prior to January 2020 (n=16) or at the University of Edinburgh (n=10) between September 2020 and January 2021. Matched (n=6) and healthy volunteers (n=10) scanned during the pandemic were eligible once previous COVID-19 infection or current symptoms of COVID-19 were excluded. The majority of this cohort (matched n=6, healthy n=8) underwent regular PCR testing during hospital admission or due to occupational requirements. Exclusion criteria for all participants included contraindications to MRI or manganese dipyridoxyl diphosphate administration (online supplemental methods).

Myocardial injury was defined as plasma cardiac troponin I concentration above the 99th centile (female: 16 ng/L, male: 34 ng/L) but was not necessary for inclusion. Quick COVID-19 severity index was used to assess severity with severe cases defined as having an index of >4 (>30% risk of critical illness) (online supplemental methods).¹⁸

Magnetic resonance imaging

MRI in Edinburgh was performed using a Siemens MAGNETOM Skyrafit 3T scanner (Siemens Healthineers, Erlangen, Germany) with a dedicated 30-channel body matrix coil. MRI in Leicester

was performed using a Siemens MAGNETOM Skyra 3T scanner (Siemens Healthineers, Erlangen, Germany) with an 18-channel cardiac coil. All study participants underwent imaging with late gadolinium enhancement. Patients from Edinburgh and all healthy volunteers underwent additional manganese-enhanced MRI, at least 48 hours apart. Patients were scanned during convalescence. Images were acquired during expiratory breath hold with ECG gating. Cine imaging was acquired with standard steady-state free precession sequences in long-axis and short-axis orientations as described previously.¹⁷ T2 mapping (MyoMaps) was acquired in the short-axis orientation covering the entire left ventricle. Native T1 mapping was acquired with a Modified Look-Locker Inversion recovery short-axis stack. Patients with COVID-19 scanned in Leicester underwent native T1 mapping with a shortened modified Look-Locker inversion recovery short-axis stack.

Late gadolinium enhancement

Late gadolinium enhancement images were acquired following intravenous gadobutrol (0.1 mmol/kg; Gadovist, Bayer, Germany)¹⁹ using a single breath hold per slice with a short-axis stack and long-axis orientations. T1 mapping was acquired prior to and 10 min postcontrast (online supplemental methods).

Manganese-enhanced MRI

Manganese-enhanced MRI was carried out using intravenous infusion of manganese dipyridoxyl diphosphate (5 µmol/kg, 1 mL/min, 0.1 mL/kg; Exova SL Pharma, Wilmington, Delaware, USA). T1 mapping was performed precontrast with a full short-axis Modified Look-Locker Inversion recovery stack, which have been described previously (online supplemental methods).¹⁷

Image analysis

Cardiovascular magnetic resonance studies were analysed offline using Circle CVI (Circle Cardiovascular Imaging, CVI42 V.5.3.6, Calgary Canada). T1, T2 maps, late gadolinium enhancement and cine-derived volumetric and functional sequences were analysed by experienced observers (MD, TS and TAK). Native T1 and T2 measurements were taken from septal segments, although we also report results for global T1. T1 mapping acquired using shortened modified Look-Locker inversion recovery was excluded from native T1 analysis but not from extracellular volume analysis. Areas of late gadolinium enhancement were included for calculating global extra cellular volume. Late gadolinium enhancement was adjudicated by consensus of expert observers (GPM and JRA) who were blinded to all participant details (including whether scans were from patients or volunteers) and classified as ischaemic or non-ischaemic (midwall or epicardial) pattern. Right ventricular insertion point enhancement in isolation was not considered pathological.

Manganese kinetic modelling

Myocardial calcium handling was assessed using T1 maps during manganese-enhanced MRI.^{20,21} Regions of interest were drawn in areas of myocardial abnormalities or the midventricular septum in those without myocardial abnormalities (mean size: $0.7 \pm 0.13 \text{ cm}^2$). The rate of myocardial manganese uptake was determined by Patlak modelling as described previously.¹⁷

CT coronary angiography (CTCA)

Patients scanned in Edinburgh underwent CTCA, which was performed with a 128-multidetector row scanner (Siemens Biograph, Siemens Healthcare, Erlangen, Germany) according

Table 1 Baseline characteristics of study populations

	Patients with COVID-19 (n=52)	Comorbidity-matched volunteers (n=26)	Healthy volunteers (n=10)	P value*	P value†
Age, median (IQR) (years)	55 (51–57)	53 (47–57)	35 (29–40)	0.58	<0.0001
Male	39 (75)	19 (73)	9 (90)		
Body mass index, median (IQR) (kg/m ²)	28 (18–42)	27 (22–41)	21 (22–27)	0.26	<0.001
Time of scan post symptoms onset median ±IQR (days)	90±(7–290)	–	–		
Persistent symptoms, n (%)	20 (38)	–	–		
Intensive care admission, n (%)	15 (29)	–	–		
Endotracheal intubation, n (%)	5 (10)	–	–		
Non-invasive ventilation, n (%)	6 (12)	–	–		
Quick COVID-19 severity index, n (%)		–	–		
Low	21 (40)		–		
Low intermediate	13 (25)		–		
High intermediate	14 (27)		–		
High	4 (8)		–		
Medical history, n (%)			–		
Hypertension	18 (35)	8 (31)	–		
Ischaemic heart disease	8 (15)	5 (19)	–		
Hypercholesterolaemia	16 (31)	8 (31)	–		
Atrial fibrillation/flutter	2 (4)	1 (4)	–		
Previous cerebrovascular event	1 (2)	0	–		
Diabetes mellitus	18 (35)	11 (38)	–		
Non-cardiac	17 (33)	2 (8)	–		
Medications, n (%)					
Antiplatelet therapy	9 (17)	6 (23)			
Beta-blocker therapy	8 (15)	4 (15)			
ACE inhibitor or angiotensin receptor blocker therapy	14 (27)	9 (35)			
Diuretic therapy	2 (4)	0			
Statin therapy	16 (31)	10 (38)			
Antiglycaemic therapy	18 (35)	11 (42)			
Smoking status, n (%)					
Non-smoker	43 (83)	14 (54)	0		
Ex-smoker	8 (15)	10 (38)	0		
Current smoker	0	1 (4)	0		

*Patients with COVID-19 versus comorbidity-matched volunteers.

†Patients with COVID-19 versus healthy volunteers.

to Society of Cardiovascular Computed Tomography guidelines and have been described previously (online supplemental methods).²²

Statistical analysis

All statistical analyses were performed with GraphPad Prism (GraphPad Software V.8.0.2, San Diego, California, USA). Categorical baseline variables were presented as number (%) and compared using χ^2 test. Continuous data were assessed for normality using the D'Agostino-Pearson test and presented as mean±SD or median (IQR). Cardiac function, myocardial manganese uptake, volumetric assessment and parametric mapping values were compared using paired or unpaired Student's t-tests, Wilcoxon or Mann-Whitney tests and ANOVA±Dunnett's as appropriate. Statistical significance was taken as two-sided $p<0.05$.

RESULTS

Study populations

Fifty-four patients recovering from COVID-19 were recruited into the study with two patients withdrawing due to problems with vascular access or claustrophobia (figure 1). Ten healthy

volunteers and 26 volunteer patients matched for age, sex and comorbidities were recruited as comparator groups (table 1).

Characteristics of patients with COVID-19

All patients with COVID-19 were symptomatic and required hospitalisation, with the the most common symptom being dyspnoea (87%) and a smaller proportion presenting with chest pain (13%). Twenty-seven (52%) patients had severe disease with a Quick COVID-19 severity score of greater than 4, 15 (29%) requiring admission to the intensive care unit and 11 (21%) undergoing non-invasive or invasive ventilation. Overall, 29 (56%) patients had pre-existing cardiovascular disease or risk factors including hypertension, diabetes mellitus and hypercholesterolaemia. Seventeen (33%) had an elevation in plasma high-sensitivity cardiac troponin I concentration above the normal upper reference limit (online supplemental table 1). Of those who underwent clinically indicated echocardiography during their hospital admission, 10 (19%) had an abnormal echocardiogram with six demonstrating right ventricular dilatation and three left ventricular dilatation (online supplemental table 2). Eight of the 10 patients with an abnormal baseline echocardiogram received either non-invasive or invasive ventilation. Of

Table 2 Coronary CT angiography findings

	Patients with COVID-19 (n=23)
Normal	15 (65)
Non-obstructive disease	7 (22)
Mild (<50%)	4 (17)
Moderate (50%–70%)	3 (13)
Obstructive disease	1 (4)
One vessel	0
Two vessels	1 (4)
Three vessels	0
Other cardiac findings	
LV thrombus	1 (4)
Anomalous coronary anatomy	1 (4)
Non-cardiac findings	
Parenchymal scarring/atelectasis	7 (30)
Peripheral ground glass opacification	2 (9)
Pulmonary mass or nodule	1 (4)
Emphysema	3 (13)
Hiatus hernia	1 (4)
Liver pathology	2 (9)
Pulmonary embolism	0

n (%).

LV, left ventricle.

those who had CT pulmonary angiography as part of clinical care (n=19), two had evidence of pulmonary emboli.

CT coronary angiography

Twenty-three patients underwent CTCA and were scanned 90 days (IQR: 7–290 days) following symptom onset. Sixty-five per cent of patients (15 of 23) had normal coronary arteries and 35% (8 of 23) had evidence of coronary artery disease with one patient having obstructive disease (table 2). Within this subgroup, eight patients (35%) described persistent dyspnoea at the time of imaging, of whom seven demonstrated persistent parenchymal lung abnormalities at the time of imaging (figure 2).

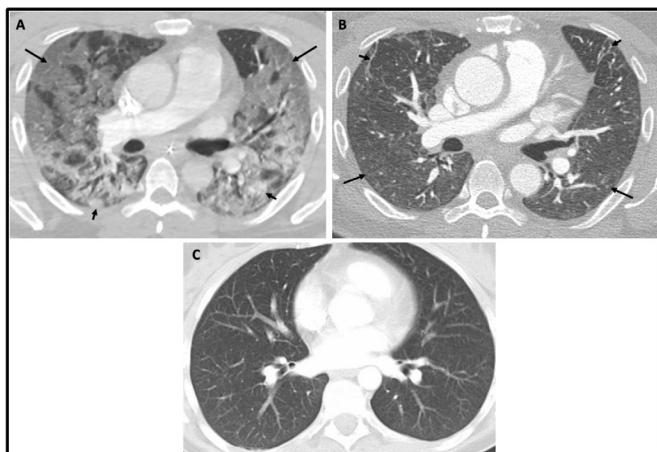


Figure 2 Chest CT in severe COVID-19. Typical COVID-19 appearance with ground glass opacification (long arrow) and peripheral basal consolidation (short arrow) on during hospital admission (A) and 4 months later (B) with residual atelectasis (short arrow) and subtle ground glass opacification (long arrow) in a patient with severe COVID-19 with ongoing symptoms compared with a patient with COVID-19 without symptoms (C).

Cardiac MRI

Patients with COVID-19 compared with healthy volunteers

In comparison with younger healthy volunteers, patients with COVID-19 had reduced biventricular systolic function (table 3). Septal native myocardial T1 values (1225±46 (95% CI 1205 to 1240) vs 1197±30 (95% CI 1178 to 1216) ms; p=0.04; figure 3), global native T1 values (table 3) and extracellular volume fraction (31±4 (95% CI 29.6 to 32.1) vs 24±3 (95% CI 33.4 to 25.4)%; p=0.0003; figure 3) were higher in patients with COVID-19. None of the healthy volunteers had evidence of late gadolinium enhancement. Manganese-enhanced MRI demonstrated reduced uptake of myocardial manganese uptake in patients recovering from COVID-19 (mean Ki 6.9±0.9 (95% CI 6.5 to 7.3) vs 7.9±1.2 (95% CI 7.4 to 8.5) mL/100 g/min; p=0.01, figure 3).

Patients with COVID-19 compared with comorbidity-matched volunteers

There were no major differences in left ventricular volumes and systolic function between patients and comorbidity-matched volunteers. However, patients recovering from COVID-19 did have reduced right ventricular systolic function (51.7±9.1 (95% CI 53.9 to 60.1) vs 59.3±4.9 (95% CI 51.0 to 66.5)%; p=0.0005, table 3). When compared with comorbidity-matched volunteers, septal native myocardial T1 values (1225±46 (95% CI 1205 to 1240) vs 1227±51 (95% CI 1208 to 1246) ms; p=0.99, figure 3), global native T1 values (table 2) and extracellular volume fraction (31±4 (95% CI 29.6 to 32.1) vs 29±5 (95% CI 27.0 to 31.2)%; p=0.35, figure 3) were similar. Myocardial manganese uptake (mean Ki 6.9±0.9 (95% CI 6.5 to 7.3) vs 7.3±1.3 (95% CI 6.7 to 7.9) mL/100 g/min; p=0.45, figure 3) was also comparable. Late gadolinium enhancement was seen in 18 (35%) patients with COVID-19, with nine demonstrating a non-ischaemic pattern and nine with an ischaemic pattern (figure 4). None of the patients with a non-ischaemic pattern of late gadolinium enhancement had a history of prior cardiac disease and all had normal T2 values at the site of late enhancement (mean T2: 40.3±3.9 ms). Only one patient with an ischaemic pattern of enhancement had elevated T2 values in the corresponding region (45 ms). The prevalence of late gadolinium enhancement was similar in the comorbidity-matched volunteers including right ventricular insertion point enhancement (table 3, online supplemental table 3).

Influence of disease severity, myocardial injury and ongoing symptoms

In patients with severe COVID-19 (27 of 52, 52%), left ventricular function was preserved compared with matched volunteers. In contrast, right ventricular systolic function was reduced (EF 52.2±10.2 (95% CI 48.1 to 56.2) vs 59.3±4.9 (95% CI 51.0 to 66.5)%; p=0.0012). Native myocardial T1 values, extracellular volume fractions, myocardial manganese uptake and prevalence of late gadolinium enhancement were similar to comorbidity-matched volunteers (figure 5, online supplemental table 4).

Similar pattern was seen in patients with COVID-19 and evidence of myocardial injury (online supplemental table 4). Native T1, extracellular volume fractions and myocardial manganese uptake were similar to comorbidity-matched volunteers (figure 5, online supplemental table 4). There was a higher prevalence of late gadolinium enhancement in this cohort compared with matched volunteers (9 of 17, 53% vs 9 of 26, 35%), with the majority demonstrating an ischaemic pattern of injury (6 of 9, 66%).

Table 3 MRI findings

	Patients with COVID-19 (n=52)	Comorbidity-matched volunteers (n=26)	Healthy volunteers (n=10)	P value*	P value†
LVEDVI, mean±SD (95% CI), (mL/m ²)	73.1±18.1 (68.1 to 78.1)	78.5±20 (67 to 81.0)	79.2±18.3 (72.6 to 43.7)	0.99	0.17
LVESVI, mean±SD (95% CI), (mL/m ²)	32.1±16.1 (27.6 to 36.4)	31.7±16.2 (26.0 to 37.9)	25.8±7.9 (22.5 to 30.1)	0.92	0.04
Stroke volume index, mean±SD (95% CI), (mL/m ²)	41.3±10.8 (38.3 to 44.1)	44.9±8.7 (40.0 to 50.4)	52.1±10.6 (46.5 to 56.3)	0.12	0.001
LV ejection fraction, mean±SD (95% CI), (%)	57.4±11.1 (54.0 to 60.1)	61.6±9.9 (56.1 to 65.2)	66.3±5.3 (62.4 to 69.8)	0.15	0.02
LV mass index, mean±SD (95% CI), (g/m ²)	53.5±11.0 (50.4 to 56.6)	56.6±12.2 (51.8 to 60.2)	55.7±15.2 (50.6 to 61.4)	0.21	0.81
RVEDVI, mean±SD (95% CI), (mL/m ²)	79.3±16.2 (74.8 to 83.8)	75.4±12.3 (70.4 to 80.4)	74.5±9.8 (68.6 to 80.4)	0.27	0.06
RVESVI, mean±SD (95% CI), (mL/m ²)	39.9±15.3 (34.7 to 43.3)	30.1±7.8 (28.2 to 33.5)	29.3±5.4 (26.1 to 32.6)	0.006	0.02
RV stroke volume index, mean±SD (95% CI), (mL/m ²)	39.8±9.7 (37.2 to 42.6)	45.1±9.8 (45.2 to 55.7)	47.5±9.3 (42.1 to 52.9)	0.02	0.01
RV ejection fraction, mean±SD (95% CI), (%)	51.7±9.1 (53.9 to 60.1)	59.3±4.9 (51.0 to 66.5)	60.5±4.9 (57.1 to 63.2)	0.0005	<0.0001
Main pulmonary artery, mean±SD (mm)	20.7±3.1	22.8±6.6	18.5±4.0	0.09	0.05
Late gadolinium enhancement pattern, n (%)	18 (35)	9 (35)	0		
Ischaemic	9 (17)	5 (19)	–		
Non-ischaemic	9 (17)	4 (15)	–		
Native T1-septum, mean±SD (95% CI), (ms)	1225±46‡ (1205 to 1240)	1227±51§ (1208 to 1246)	1197±30 (1178 to 1216)	0.99	0.04
Global T1- midventricular, mean±SD (95% CI), (ms)	1210±38‡ (1193 to 1226)	1208±33§ (1191 to 1228)	1184±24 (1168 to 1200)	0.88	0.04
Extracellular volume, mean±SD (95% CI), (%)	31±4 (29.6 to 32.1)	29±5 (27.0 to 31.2)	24±3 (22.4 to 26.4)	0.35	0.0003
T2 septum, mean±SD (95% CI), (ms)	37.3±4.6 (35.9 to 38.6)	38.5±5.9 (36.1 to 40.1)	38.7±3 (37.4 to 40.1)	0.35	0.18
Manganese influx constant, mean±SD (95% CI), (Ki/mL/100 g/min)	6.9±0.9‡ (6.5 to 7.3)	7.3±1.3§ (6.7 to 7.9)	7.9±1.2 (7.4 to 8.5)	0.45	0.01

Bold values are statistically significant (<0.05).

*Patients with COVID-19 versus comorbidity-matched volunteers.

†Patients with COVID-19 versus healthy volunteers.

‡n=23.

§n=20.

LV, left ventricular; LVEDVI, indexed left ventricular end-diastolic volume; LVESVI, indexed left ventricular end-systolic volume; RV, right ventricular; RVEDVI, indexed right ventricular end-diastolic volume; RVESVI, indexed right ventricular end-systolic volume.

Twenty of 52 patients (38%) had ongoing symptoms at the time of scanning. While these patients had comparable left ventricular systolic function to matched volunteers, they had reduced right ventricular systolic function (EF 49.0±6.5 (95% CI 45.9 to 52.2) vs 59.3±4.9 (95% CI 51.0 to 66.5)%; $p<0.0001$; figure 5, online supplemental table 4). Native T1 values, extracellular volume fractions, myocardial manganese uptake and prevalence of late gadolinium enhancement were similar to comorbidity-matched volunteers (online supplemental table 4).

DISCUSSION

In this prospective multimodality two-centre observational study, we have shown that patients recovering from severe COVID-19 do not have evidence of left ventricular dysfunction or a major excess in persistent myocardial injury compared with comorbidity-matched volunteers. These patients have a high prevalence of cardiovascular comorbidity that may account for much of the reported myocardial abnormalities on cardiac magnetic resonance. However, some patients recovering from COVID-19 did have evidence of mild persistent right ventricular dysfunction that likely reflects recovery from a severe life-threatening respiratory viral illness. It is possible that the cardiac consequences of COVID-19 may relate to the severity of the

pulmonary effects of COVID-19 rather than direct cardiac effects of COVID-19 infection.

Several studies have reported cardiac abnormalities on cardiac MRI in patients who have recovered from COVID-19. These range from elevated native T1 and T2 values, to presence of cardiac dysfunction and late gadolinium enhancement.^{8 10–13 23–25} Raman and colleagues²⁵ described myocardial injury in a third of patients with moderate to severe COVID-19, but they lacked a well-matched control population. Huang and colleagues¹⁰ described abnormalities in 58% patients who had recently recovered from COVID-19 with ongoing cardiac symptoms although only a third of cases had evidence of late gadolinium enhancement. Similarly, Puntmann and colleagues¹¹ suggested that 70% of patients with COVID-19 have ongoing cardiac damage, with 32% of patients having late gadolinium enhancement and the majority having elevations in native T1 values or extracellular volume fraction. However, native T1 values vary between individuals and are affected by comorbidities, such as hypertension and diabetes mellitus.^{26 27} It is therefore not surprising that while we observed increased native T1 values in patients with COVID-19, these differences disappeared once comparisons were made with comorbidity-matched volunteers. Similar observations were made for extracellular volume fraction, T2 mapping and

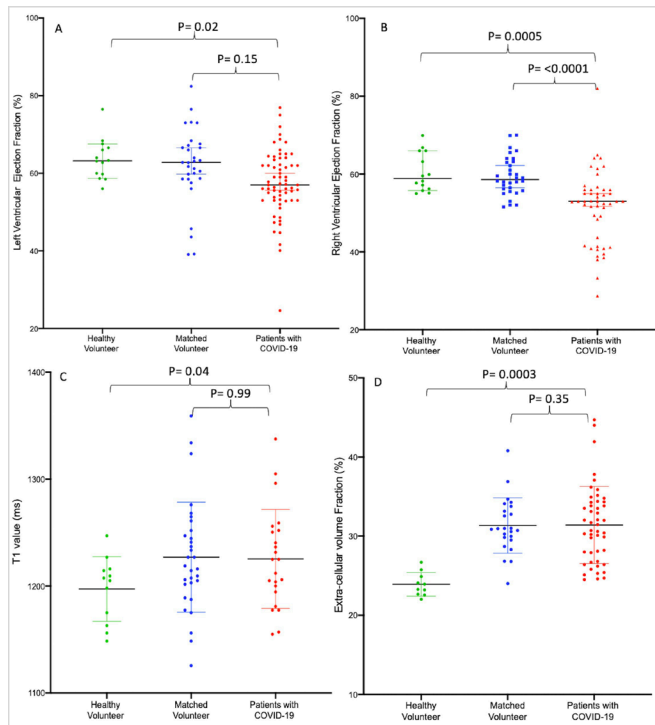


Figure 3 Cardiac MRI in patients with COVID-19 compared with matched volunteers and healthy volunteers. Left ventricular (LV) ejection fraction (A), right ventricular (RV) ejection fraction (B), native T1 values (C) and extracellular volume (D) in healthy control volunteers (n=10, green), matched control volunteers (n=26, blue) and patients with COVID-19 (n=52, red).

manganese assessments of myocyte function indicating that differences in these measures may relate to underlying comorbidities rather than persistent damage or injury from COVID-19. Similar to previous studies,^{11,25} a third of our cohort demonstrate late gadolinium enhancement, which was comparable with our

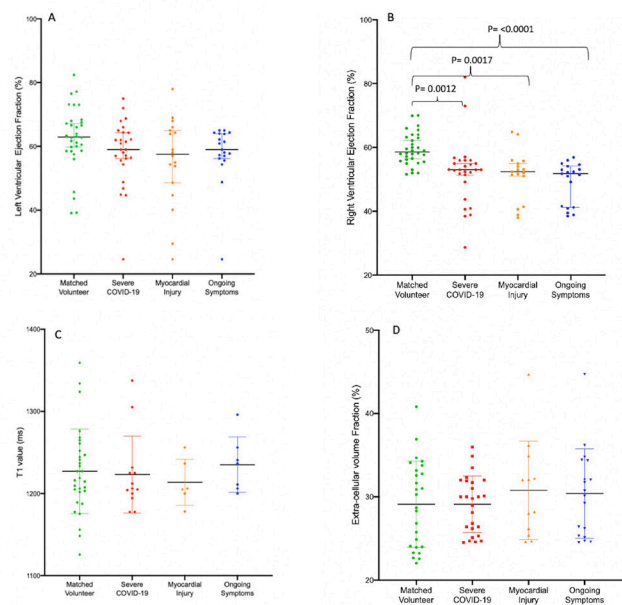


Figure 5 Cardiac MRI in subgroups of patients with COVID-19 compared with matched volunteers. Left ventricular (LV) ejection fraction (A), right ventricular (RV) ejection fraction (B), native T1 values (C) and extracellular volume (D) in matched control volunteers (n=26, green) and patients with COVID-19 and severe COVID-19 disease (n=27, red), myocardial injury (n=17, orange) or ongoing symptoms (n=20, blue).

comorbidity-matched volunteer group, which included those with coronary artery disease. This begs the question whether individuals with cardiovascular risk factors, who are at higher risk of developing severe COVID-19, demonstrate late gadolinium enhancement as a result of their pre-existing conditions rather than COVID-19 itself.

Cardiac Magnetic Resonance features in Hospitalised COVID-19 survivors

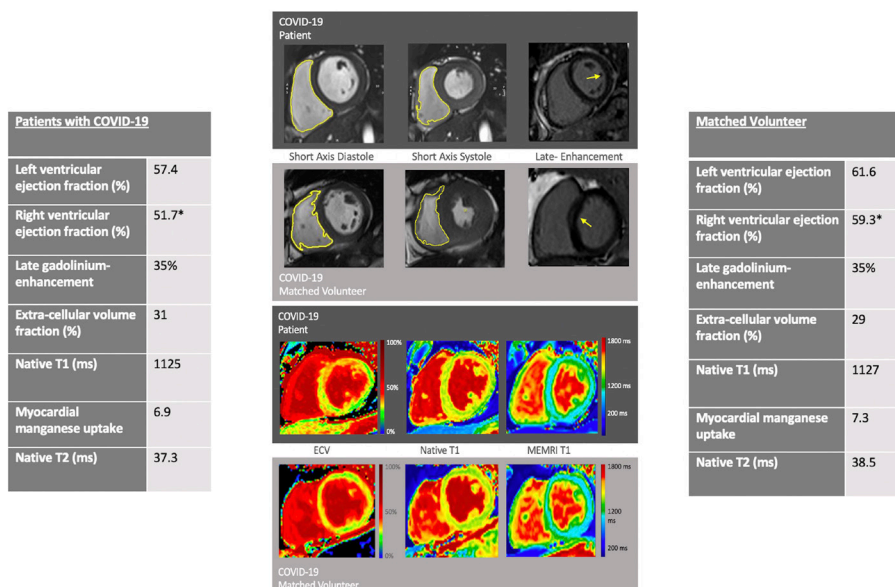


Figure 4 Cardiac magnetic resonance features in hospitalised COVID-19 survivors. MRI findings in patients recovering from COVID-19 infection compared with age, sex and comorbidity matched volunteers. *Statistically significant.

Kotecha and colleagues⁸ described similar native T1 and T2 values in COVID-19 survivors and comorbidity-matched volunteers. However, they demonstrated a higher rate of late gadolinium enhancement (49%) in patients with COVID-19 compared with our study and their matched control group. However, all their patients had elevated cardiac troponin concentrations and had been referred for cardiac MRI for clinical indications. Both factors will have introduced a case selection bias that will likely have increased their rate of late gadolinium enhancement. It has been suggested that non-ischaemic late gadolinium enhancement could represent COVID-19 related myocarditis, although without evidence on corresponding oedema imaging during the acute illness or other forms of validation, this cannot be established. An inflammatory cardiomyopathy has previously been linked with several viruses including influenza²⁸ but its association with COVID-19 remains unclear. Moreover, similar patterns of non-ischaemic late gadolinium enhancement are commonly observed in patients with hypertension and diabetes mellitus²⁷ in the absence of myocarditis. Regardless of the mechanism, the prognostic value of late gadolinium enhancement across multiple disease states probably warrants long-term follow-up.

Similar to previous studies,^{8, 11} we observed that patients had evidence of increased right ventricular dysfunction, particularly in those with severe COVID-19, myocardial injury and ongoing symptoms. Development of pulmonary fibrosis in severe acute respiratory syndrome coronavirus-1 and adult respiratory distress syndrome have been reported in patients during recovery. Given SARS-CoV-2 affinity for lung and heart tissues, it is possible severe lung injury in the setting of SARS-CoV-2 infection may lead to pulmonary fibrosis and elevated pulmonary pressure. These are all risk factors for the development of right ventricular dysfunction.²⁹ Furthermore, the persistence of symptoms in our patient cohort also related to persistent lung abnormalities observed on CT. However, due to the study size, this cannot be assumed, and further research should focus on patients with persistent symptoms.

We should consider the strengths and weaknesses of our study. We have undertaken a thorough assessment of cardiac structure and function with the use of multiple imaging modalities. While echocardiography is more practical and most widely used clinically, we chose to use contrast-enhanced cardiac MRI to identify and to characterise any myocardial abnormalities since it is the most sensitive non-invasive measure to achieve this. Importantly, images were analysed by readers blinded to participant details and COVID-19 status, a rigorous approach that was not always applied in previous studies. Manganese-enhanced MRI is a novel and sensitive measure of myocyte function,^{17, 20} which allowed us to assess subtle changes alongside more traditional assessments of cardiac function. The use of CT coronary angiography also allowed assessment of both coronary artery disease and the presence of persistent lung damage. Despite this, we observed no left ventricular dysfunction when compared with appropriate comparator groups.

This study is limited by its modest sample size and the heterogeneity of patients surviving COVID-19. However, we have focused on the patient cohort of most interest, patients recovering following hospitalisation with severe COVID-19. Other limitations of our study include the use of evolving therapeutic interventions and, perhaps more importantly, survival bias. As the pandemic evolved, new therapeutic interventions, such as dexamethasone, were introduced to reduce mortality, and this could also have influenced our findings. Over half of the patients who were eligible for the study died, and it is certainly possible that more extensive abnormalities could have been observed

had earlier imaging been possible in these patients. As a consequence, our findings are limited to the population of patients who recover from severe COVID-19. It is difficult to ascertain whether the abnormalities seen in patients with COVID-19 were present prior to hospitalisation; however, it is reassuring that there was no excess in left ventricular abnormalities when compared with matched volunteers. Lastly, in an ideal world, a comparator group should include patients with non-COVID-19 viral or bacterial pneumonitis patients with a similar incidence of intensive care admissions, and this is an area for future studies to focus on.

In conclusion, concomitant comorbidities and risk factors play a major role in prior reports of left ventricular abnormalities associated with COVID-19. In patients who recovered from severe COVID-19, there was evidence of persistent right ventricular dysfunction that presumably reflects the recent severe viral pneumonia and consequent pulmonary hypertension.

Key messages

What is already known on this subject??

- ▶ There is major interest in the cardiac consequences of COVID-19, and it is essential to establish the true impact of COVID-19 and how it will affect healthcare in the years to follow.

What might this study add??

- ▶ This study shows that the consequences of abnormalities seen on cardiac MRI in patients with COVID-19 remain unclear. Many abnormalities may be attributable to comorbidity and concomitant cardiovascular risk factors rather than COVID-19 per se. Right ventricular abnormalities do occur and likely reflect the consequences of a severe viral pneumonia.

How might this impact on clinical practice?

- ▶ Further research is needed to establish the true extent of cardiac abnormalities in patients who have suffered severe COVID-19 and to determine whether this is likely to impact on their long-term clinical outcome.

Author affiliations

¹BHF Centre for Cardiovascular Science, The University of Edinburgh, Edinburgh, UK
²Cardiovascular Science, Edinburgh Heart Centre, Royal Infirmary of Edinburgh, Edinburgh, UK

³Edinburgh Imaging Facility, Queens Medical Research Institute, University of Edinburgh, Edinburgh, UK

⁴Department of Cardiovascular Sciences, University of Leicester and NIHR Leicester Biomedical Research Centre, Glenfield Hospital, Leicester, UK

⁵Centre for Inflammation Research, University of Edinburgh, Edinburgh, UK

⁶Department of Anaesthesia, Critical Care and Pain Medicine, Royal Infirmary of Edinburgh, Edinburgh, UK

Correction notice This article has been corrected since it was first published. To correct the readability, multiple full-stops have been changed to commas in the Abstract and the Results section.

Twitter Thomas A Kite @drtomkite and Michelle Claire Williams @imagingmedsci

Acknowledgements Grateful acknowledgements are made to the Edinburgh Imaging Facility and Glenfield Hospital radiographers.

Contributors Author contributions are as follows: TS, SIKS, DEN and MD conceived and designed the study; TS and TAK recruited and scanned all patients, performed kinetic modelling and compiled the original manuscript; TS, TAK, MD, GPM, JRA, MCW and EJRvB were involved in data analysis; LK wrote and validated the code for kinetic modelling; SJ, NBS, LK, AB, HJ, SIKS, MD, DEN and GPM contributed revision and critical appraisal of the final manuscript for important intellectual content. All authors approved the final manuscript submitted. TS and TAK contributed equally.

Funding This work and TS, TAK, SJ, MD, MCW and DEN are supported by the British Heart Foundation (FS/17/19/32641, CS/17/1/32445, FS/14/78/31020, CH/09/002, RG/16/10/32375, RE/18/5/34216, FS/ICRF/20/26002). TS is supported by the MRC (MR/T029153/1). MCW is supported by The Chief Scientist Office of the Scottish Government Health and Social Care Directorates (PCL/17/04). DEN is the recipient of a Wellcome Trust Senior Investigator Award (WT103782AIA). GPM and JRA are supported by the National Institute for Health Research (NIHR) research professorship (RP-2017–08-ST2-007) and Clinician Scientist Award (CS-2018–18-ST2-007) respectively and receive support from the NIHR Leicester Biomedical Research Centre. AJM is supported by a BHF Accelerator Award (AA/18/3/34220). The Edinburgh Clinical Research Facilities and Edinburgh Imaging facility is supported by the National Health Service Research Scotland (NRS) through National Health Service Lothian Health Board. Patients in Leicester were scanned in the NIHR Leicester Clinical Research Facility.

Disclaimer DEN and SIKS hold unrestricted educational grants from Siemens Healthineers. GPM holds a research agreement with Circle CVI.

Competing interests None declared.

Patient consent for publication Not applicable.

Ethics approval This was a prospective observational study, which was conducted in accordance with the Declaration of Helsinki, with favourable ethical opinion from South East Scotland Research Ethics Committee 2 (20/SS/0001).

Provenance and peer review Not commissioned; externally peer reviewed.

Data availability statement Data may be available on reasonable request. All data relevant to the study are included in the article or uploaded as supplementary information.

Supplemental material This content has been supplied by the author(s). It has not been vetted by BMJ Publishing Group Limited (BMJ) and may not have been peer-reviewed. Any opinions or recommendations discussed are solely those of the author(s) and are not endorsed by BMJ. BMJ disclaims all liability and responsibility arising from any reliance placed on the content. Where the content includes any translated material, BMJ does not warrant the accuracy and reliability of the translations (including but not limited to local regulations, clinical guidelines, terminology, drug names and drug dosages), and is not responsible for any error and/or omissions arising from translation and adaptation or otherwise.

Open access This is an open access article distributed in accordance with the Creative Commons Attribution Non Commercial (CC BY-NC 4.0) license, which permits others to distribute, remix, adapt, build upon this work non-commercially, and license their derivative works on different terms, provided the original work is properly cited, appropriate credit is given, any changes made indicated, and the use is non-commercial. See: <http://creativecommons.org/licenses/by-nc/4.0/>.

ORCID iDs

Trisha Singh <http://orcid.org/0000-0002-4314-9935>
 Thomas A Kite <http://orcid.org/0000-0002-6021-5738>
 Shruti S Joshi <http://orcid.org/0000-0001-9874-6211>
 Nick B Spath <http://orcid.org/0000-0001-9623-0158>
 Michelle Claire Williams <http://orcid.org/0000-0003-3556-2428>
 Alastair James Moss <http://orcid.org/0000-0003-4123-2070>
 David E Newby <http://orcid.org/0000-0001-7971-4628>
 Gerry P McCann <http://orcid.org/0000-0002-5542-8448>

REFERENCES

- Zhou F, Yu T, Du R, *et al*. Clinical course and risk factors for mortality of adult inpatients with COVID-19 in Wuhan, China: a retrospective cohort study. *Lancet* 2020;395:1054–62.
- Clerkin KJ, Fried JA, Raikhelkar J, *et al*. COVID-19 and cardiovascular disease. *Circulation* 2020;141:1648–55.
- Guo T, Fan Y, Chen M, *et al*. Cardiovascular implications of fatal outcomes of patients with coronavirus disease 2019 (COVID-19). *JAMA Cardiol* 2020;5:811–8.
- Smeeth L, Thomas SL, Hall AJ, *et al*. Risk of myocardial infarction and stroke after acute infection or vaccination. *N Engl J Med* 2004;351:2611–8.
- Lindner D, Fitzek A, Bräuningner H, *et al*. Association of cardiac infection with SARS-CoV-2 in confirmed COVID-19 autopsy cases. *JAMA Cardiol* 2020;5:1281–5.
- Hu H, Ma F, Wei X, *et al*. Coronavirus fulminant myocarditis treated with glucocorticoid and human immunoglobulin. *Eur Heart J* 2021;42:206.
- McCracken IR, Saginc G, He L, *et al*. Lack of evidence of angiotensin-converting enzyme 2 expression and replicative infection by SARS-CoV-2 in human endothelial cells. *Circulation* 2021;143:865–8.
- Kotecha T, Knight DS, Razvi Y, *et al*. Patterns of myocardial injury in recovered troponin-positive COVID-19 patients assessed by cardiovascular magnetic resonance. *Eur Heart J* 2021;42:1–13.
- Pellegrini D, Kawakami R, Guagliumi G, *et al*. Microthrombi as a major cause of cardiac injury in COVID-19: a pathologic study. *Circulation* 2021;143:1031–42.
- Huang L, Zhao P, Tang D, *et al*. Cardiac involvement in patients recovered from COVID-2019 identified using magnetic resonance imaging. *JACC Cardiovasc Imaging* 2020;13:2330–9.
- Puntmann VO, Carerj ML, Wieters I, *et al*. Outcomes of cardiovascular magnetic resonance imaging in patients recently recovered from coronavirus disease 2019 (COVID-19). *JAMA Cardiol* 2020;5:1265.
- Knight DS, Kotecha T, Razvi Y, *et al*. COVID-19: myocardial injury in survivors. *Circulation* 2020;142:1120–2.
- Starekova J, Bluemke DA, Bradham WS, *et al*. Evaluation for myocarditis in competitive student athletes recovering from coronavirus disease 2019 with cardiac magnetic resonance imaging. *JAMA Cardiol* 2021;6:945.
- Buzon J, Roignot O, Lemoine S, *et al*. Takotsubo cardiomyopathy triggered by influenza A virus. *Intern Med* 2015;54:2017–9.
- Ayoubkhani D, Khunti K, Nafilyan V. Epidemiology of post-COVID syndrome following hospitalisation with coronavirus: a retrospective cohort study. *medRxiv* 2021;27:601–15.
- Nalbandian A, Sehgal K, Gupta A, *et al*. Post-Acute COVID-19 syndrome. *Nat Med* 2021;27:601–15.
- Spath NB, Singh T, Papanastasiou G, *et al*. Manganese-Enhanced magnetic resonance imaging in dilated cardiomyopathy and hypertrophic cardiomyopathy. *Eur Heart J Cardiovasc Imaging* 2020;jeaa273.
- Haimovich AD, Ravindra NG, Stoytchev S, *et al*. Development and validation of the quick COVID-19 severity index: a prognostic tool for early clinical decompensation. *Ann Emerg Med* 2020;76:442–53.
- Papanastasiou G, Williams MC, Kershaw LE, *et al*. Measurement of myocardial blood flow by cardiovascular magnetic resonance perfusion: comparison of distributed parameter and Fermi models with single and dual bolus. *J Cardiovasc Magn Reson* 2015;17:17.
- Spath NB, Lilburn DML, Gray GA, *et al*. Manganese-Enhanced T₁ Mapping in the Myocardium of Normal and Infarcted Hearts. *Contrast Media Mol Imaging* 2018;2018:1–13.
- Nick S, Trisha S, Giorgos P. Manganese-Enhanced T1 mapping in Non-Ischaemic cardiomyopathy. *J Am Coll Cardiol* 2020;75.
- Abbara S, Blanke P, Maroules CD, *et al*. SCCT guidelines for the performance and acquisition of coronary computed tomographic angiography: a report of the Society of Cardiovascular Computed Tomography guidelines Committee: endorsed by the North American Society for cardiovascular imaging (NASCI). *J Cardiovasc Comput Tomogr* 2016;10:435–49.
- Hays GA SH. The heart of the pandemic: insights of CMR imaging in COVID-19. *Am Coll Cardiol* 2020.
- Ojha V, Verma M, Pandey NN, *et al*. Cardiac magnetic resonance imaging in coronavirus disease 2019 (COVID-19): a systematic review of cardiac magnetic resonance imaging findings in 199 patients. *J Thorac Imaging* 2021;36:73–83.
- Raman B, Cassar MP, Tunnicliffe EM, *et al*. Medium-Term effects of SARS-CoV-2 infection on multiple vital organs, exercise capacity, cognition, quality of life and mental health, post-hospital discharge. *EClinicalMedicine* 2021;31:100683.
- Rodrigues JCL, Amadu AM, Dastidar AG, *et al*. Comprehensive characterisation of hypertensive heart disease left ventricular phenotypes. *Heart* 2016;102:1671–9.
- Shang Y, Zhang X, Leng W, *et al*. Assessment of diabetic cardiomyopathy by cardiovascular magnetic resonance T1 mapping: correlation with left-ventricular diastolic dysfunction and diabetic duration. *J Diabetes Res* 2017;2017:1–8.
- Mavrogeni S, Bratis C, Kitsiou A, *et al*. CMR assessment of myocarditis in patients with cardiac symptoms during H1N1 viral infection. *JACC Cardiovasc Imaging* 2011;4:307–9.
- Venkataraman T, Frieman MB. The role of epidermal growth factor receptor (EGFR) signaling in SARS coronavirus-induced pulmonary fibrosis. *Antiviral Res* 2017;143:142–50.